Computational Identification of a p38^{SAPK}-Regulated Transcription Factor Network Required for Tumor Cell Quiescence

Alejandro P. Adam,[2] Ajish George,[1,2] Denis Schewe,[1,2] Paloma Bragado,[1] Bibiana V. Iglesias,[2] Aparna C. Ranganathan,[1,2] Antonis Kourtidis,[2] Douglas S. Conklin,[2] and Julio A. Aguirre-Ghiso[1,2]

[1]Division of Hematology and Oncology, Department of Medicine and Department of Otolaryngology, Mount Sinai School of Medicine, New York, New York and [2]Department of Biomedical Sciences, School of Public Health and Center for Excellence in Cancer Genomics, SUNY-Albany, Rensselaer, New York

Abstract

The stress-activated kinase p38 plays key roles in tumor suppression and induction of tumor cell dormancy. However, the mechanisms behind these functions remain poorly understood. Using computational tools, we identified a transcription factor (TF) network regulated by p38α/β and required for human squamous carcinoma cell quiescence *in vivo*. We found that p38 transcriptionally regulates a core network of 46 genes that includes 16 TFs. Activation of p38 induced the expression of the TFs p53 and BHLHB3, while inhibiting c-Jun and FoxM1 expression. Furthermore, induction of p53 by p38 was dependent on c-Jun down-regulation. Accordingly, RNAi down-regulation of BHLHB3 or p53 interrupted tumor cell quiescence, while down-regulation of c-Jun or FoxM1 or overexpression of BHLHB3 in malignant cells mimicked the onset of quiescence. Our results identify components of the regulatory mechanisms driving p38-induced cancer cell quiescence. These may regulate dormancy of residual disease that usually precedes the onset of metastasis in many cancers. [Cancer Res 2009;69(14):5664–72]

Introduction

The stress-activated protein kinase p38 is an evolutionarily conserved pathway involved in inflammation, apoptosis, and stress signaling (1). In mammals, there are four p38 isoforms encoded by different genes (α, β, γ, and δ; ref. 1). The best functionally characterized isoforms are p38α and p38β (1). Deletion of p38α is embryonic lethal in mice due to problems with placental development.

Activation of p38 is required for suppression of oncogene-induced transformation and tumorigenesis (1). These functions depend in part on p53, the cellular senescence pathway and the regulation of genes important for G_1-S and G_2-M checkpoints (1–3). Several tumors overexpress the p38 phosphatase WIP1, suggesting that down-regulation of p38 is important to allow tumor progression (2). Furthermore, conditional deletion of p38α in lungs and livers favors unscheduled proliferation of progenitor cells and tumor formation through enhanced c-Jun-NH_2-kinase and c-Jun signaling in mice (4, 5). Although increased p38 activity may be advantageous for tumor cells in highly advanced cancers (6), in some instances, tumors cells may still be susceptible to the negative regulation of p38 (7–11). For instance, MKK4 mediates suppression of metastases in ovarian cancer via activation of p38 (10).

Metastatic squamous carcinoma HEp3 cells (T-HEp3) adapted to the *in vitro* microenvironment for >40 generations reprogram and lose their tumorigenic and metastatic potential *in vivo* (9, 12). Loss of malignancy is not due to enhanced apoptosis, but due to a G_0-G_1 arrest that leads to the acquisition of a dormant phenotype upon reinoculation *in vivo* (13). This phenotype is also not due to selection of preexistent "dormancy-predisposed" clones as it happens in multiple clones isolated from HEp3 tumors at almost 100% cloning efficiency (12). Furthermore, the dormant phenotype is transient because after ~11 weeks *in vivo*, all individual clones or polyclonal tumor cell populations resumed growth (12). Cells from these tumors when placed *in vitro* can once more adopt a dormant behavior, suggesting that epigenetic mechanisms might drive this reversible dormancy behavior (12).

We hypothesized that if tumor cell dormancy does not result from the appearance of rare clones, then an epigenetic reprogramming might be responsible for the phenotypic shift. Previous studies revealed that loss of malignancy of HEp3 cells is due to the activation of p38, which inhibits extracellular signal-regulated kinase (ERK) signaling, causing a down-regulation of the urokinase receptor (uPAR) and reduced *trans*-activation of epidermal growth factor receptor (13). Genetic or pharmacologic inhibition of p38 was sufficient to restore ERK activation, uPAR expression, and proliferation of these cells *in vivo* (8, 9). In addition to HEp3 cells, activation of p38 was also predictive of proliferation versus growth arrest in breast, prostate, and fibrosarcoma cancer cell lines (7). Furthermore, independent studies showed that in malignant cervical carcinoma HeLa cells, p38 activation suppresses their tumorigenicity (11). However, the global changes in gene expression responsible for such phenotypic outcomes were unknown.

Here, we have combined gene expression profiling with a powerful bioinformatics analysis to provide a systems view of p38 and the transcription factor (TF) network signaling it regulates in dormant HEp3 cells. We identified a putative TF network using data from conventional gene array platforms and through *in vivo* validation and found that it was predictive of gene function in dormant HEp3 cells. Using this approach, we discovered that p38-induced tumor cell quiescence is controlled in part by the regulation of TFs including R213Q mutant p53, BHLHB3, Jun, and FoxM1. These results provide insight into the mechanisms by

Note: Supplementary data for this article are available at Cancer Research Online (http://cancerres.aacrjournals.org/).

A.P. Adam and A. George contributed equally to this work.

Current address for A.P. Adam: Center for Cardiovascular Sciences, Albany Medical College, Albany, NY 12208. Bibiana V. Iglesias: Center for Immunology & Microbial Disease, Albany Medical College, Albany, NY 12208. Denis Schewe: Kinderklinik und Kinderpoliklinik, Dr. von Haunersches Kinderspital, Ludwig-Maximilians-Universität, Lindwurmstr. 2, 80337 München.

Requests for reprints: J.A. Aguirre-Ghiso, Division of Hematology and Oncology, Departments of Medicine and Otolaryngology, Mount Sinai School of Medicine, New York, NY, 10029. Phone: 212-241-4096; Fax: 212-241-4096, ext. 1079; E-mail: julio.aguirre-ghiso@mssm.edu.

doi:10.1158/0008-5472.CAN-08-3820

which stress signaling might reprogram tumor cells to acquire a quiescence program and may help identify genetic determinants of cancer cell dormancy.

Materials and Methods

Reagents, siRNAs, and antibodies. SB203580, SB202190, and PD98059 were from Calbiochem. Doxorubicin and DMSO were from Sigma. Rabbit polyclonal anti-p53 and anti-Bax antibodies were from Cell Signaling; rabbit polyclonal anti c-Jun (H-79) and FoxM1 (C-20) and mouse monoclonal anti–phospho-Erk (E-4) were from Santa Cruz Biotechnology. Anti–Erk, anti-HA, anti-V5, anti–phospho-p38, and anti p38α monoclonal antibodies were from BD Biosciences. Horseradish peroxidase (HRP)–conjugated anti-mouse IgG and anti-rabbit IgG antibodies were from Vector Laboratories and Chemicon International, respectively. siRNAs to p38α were from Ambion (p38α-1) and New England Biolabs (p38α-2); siRNAs to p38β and DEC2 were from Santa Cruz Biotechnology; siRNA to c-Jun and custom FoxM1 siRNA were from Dharmacon; control and glyceraldehyde-3-phosphate dehydrogenase (GAPDH) siRNAs were from Ambion.

Cell lines and xenograft studies. Tumorigenic (T-HEp3) and "spontaneous" dormant (D-HEp3) human epidermoid carcinoma HEp3 cell (8), D-HEp3-neo, and D-HEp3-p38 DN cell lines were described previously (9). Tumor growth on chick embryo CAMs or BALB/c nude mice has been described previously (8). All animal experiments were approved by Institutional Animal Care and Use Committee (SUNY-Albany and MSSM).

Microarray analysis and TF network mapping. A total of 20 Affymetrix Hgu133a gene chips were run with the following samples: four SB203580 treatments (5 μmol/L; 48 h) and four DMSO controls, three SB202190 treatments (5 μmol/L; 48 h) and three DMSO controls, and 3 DNp38α expressing D-HEp3 cells and three empty vector (Neo) expressing D-HEp3 cells. Raw CEL file data from Affymetrix GeneChip Operating Software (GCOS) was imported into a Bioconductor session using the *Affymetrix* package (Supplementary Fig. S1). The batch was background corrected, normalized, and summarized using both gcrma and mas5 functions in parallel. Linear models of differential expression were fit to each of the transformed data sets, and contrasts were estimated between each group of p38-inhibited samples and its corresponding set of controls. Probability values of the F-statistic were used to gauge the likelihood a gene was significantly differentially expressed (Supplementary Fig. S1). The distributions of the F-statistic *P* value as determined by the classify TestsF function of the *limma* package (8) were examined, and a cutoff of significance was established at the inflection point of 0.05 occurring in both transformed sets. Genes significant in both MAS5 and gcRMA sets at this level were marked as a low-stringency group. The response of each gene in each contrast (SB203580, SB202190, and DNp38α) was then calculated using the same *P* value of 0.05 for a cutoff and a response matrix with values −1 (repressed by p38), 0 (no change), and +1 (induced by p38) was created. Response matrices for gcrma and mas5 data sets were merged to show only common responses. Genes significantly changing here in all three treatments were marked as a high-stringency group. Tables of differentially expressed genes in each list were generated (Supplementary Fig. S1).

TF network mapping. A database of known and predicted interactions between TFs and target gene promoters was developed using the TRANSFAC and LocusLink as described in Tuck and colleagues (8) and mapped to Affymetrix identifiers using Bioconductor's hgu133a package. For each combination of a TF T and a gene G present on the array: first, the scores for all known or potential binding sites for T in the promoter of G were summed up as the coregulation score; next, the nonparametric Spearman correlation between T and G across all samples was taken as the coexpression score; and finally, the coregulation and coexpression scores were multiplied together to obtain a combined score whose magnitude reflects the strength of both the coregulation and coexpression scores and whose sign reflects correlation or anticorrelation (and by extension transcriptional induction or repression; Supplementary Fig. S1). This inferred transcriptional regulation network was examined across different thresholds of the combined score for both the high and low stringency responder gene sets and including or excluding TFs that were not in the responsive gene sets. Networks that proved unmanageable for a given threshold were further filtered to include only TFs.

RNA interference studies. Retroviral delivery of shRNAs targeting the genes of interest (Open Biosystems) or, firefly luciferase or an empty vector, as control and the development of stable cell lines was done as previously described (14). Transfections of siRNAs targeting the desired sequences or, as controls, a siRNA targeting GAPDH or scrambled siRNA, were performed as previously described (14). Cells were either used for *in vivo* experiments or lysed 24 to 72 h later for immunobloting and/or qPCR.

Immunoblotting, reverse transcription-PCR, and quantitative PCR. Immunobloting and reverse transcription-PCR (RT-PCR) were performed as described previously (14). Two micrograms of total RNA isolated from HEp3 cells (Trizol reagent; Invitrogen) were reverse-transcribed using MMuLV RT (Northeast B) and then amplified by standard PCR using Taq DNA polymerase (NEB) following manufacturer's instructions. Primers were purchased from IDT. Primer sequences were as follows: GAPDH-F, CGTCATGGGTGTGAACCATGAG; GAPDH-R, GTAGACGGCAGGTCAGGTCCA; p38α-F, GCATAATGGCCGAGCTGTTGACTGG; p38α-R, AAGGGCTTGGGCCGCTGTAATTCTCT; p38β-F, GCCTGGAGATTGAGCAGTGAGGTG; p38β-R, GACACTTGTGCCCAGACTCCTACAC; p38γ-F, AGCTGAAGATCCTGGACTTCGGCC; p38γ-R, GGGAGGCCCTTCATGTAGTTCTTGG; p38δ-F, AGCAGCCGTTTGATGATTCCTTAGAAC; p38δ-R, TTTGGTAGTGACAAATACTGGTCCTTG; BHLHB3-F, ACGGAGGTTCAAGCAGAGTGAGAA; BHLHB3-R, TCAGCCACAGAACAGACCCTTCTT; p53-F, GCCCCTCCTCAGCATCTTATCCG; p53-R, TCCCAGGACAGGCACAAACACGC; cJun-F, TTAACAGTGGGTGCCAACTCATGCTAACGC; cJun-R, GAGATCGAATGTTAGGTCCATGCAGTTCTTG; FoxM1-F, GCAGCAGGCTGCACTATCAACAAT; FoxM1-R, TTCCCTGGTCCTGCAGAAGAAAGA.

Luciferase reporter assays. *In vitro* and *in vivo* dual luciferase assays were performed using the Dual Luciferase Reporter kit (Promega) following the vendor's instructions as described previously (7).

Statistical analysis. *In vivo* assays were evaluated by the nonparametric tests Mann-Whitney or Kruskal-Wallis followed by Dunn's multiple comparison test. Luciferase assays were evaluated by ANOVA followed by Bonferroni multiple comparison tests. A P value of <0.05 was considered statistically significant.

Results

Identification of a putative TF network embedded in the $p38^{SAPK}$-regulated gene expression profile. We showed that dormant D-HEp3 cells have higher P-p38 and P-Hsp27 levels than tumorigenic T-HEp3 cells (Supplementary Fig. S2). Furthermore, pharmacologic or genetic inhibition of p38α/β signaling with SB203580 or SB202190 (Supplementary Fig. S2) or dominant negative p38α(DNp38) caused a reversion of quiescence *in vivo* (7–9). Similar results were obtained with two different siRNA or shRNAs targeting p38α (Supplementary Fig. S2). Furthermore, activation of p38 signaling in T-HEp3 cells using an MMK6 active mutant inhibited T-HEp3 cell proliferation *in vivo*, mimicking the induction of dormancy (Supplementary Fig. S2). Of note is the fact that ~75% of the genes that p38 induced in D-HEp3 are also induced in D-HEp3 versus T-HEp3 cells and 97% of the genes down-regulated by p38 in D-HEp3 cells were lower in expression levels in D-HEp3 than in T-HEp3 cells (data not shown). This suggests that majority of the genes induced or repressed by p38 are also similarly regulated between T-HEp3 and D-HEp3 cells. Thus, we used this model of forced inhibition of p38 to reveal the gene program driving D-HEp3 tumor cell quiescence *in vivo*.

We compared using Affymetrix gene array profiling the gene expression changes of cells treated with or without p38 pharmacologic inhibitors SB203580 or SB202190 (5 μmol/L) for 48 h in the absence of fetal bovine serum or a genetic approach comparing D-HEp3 cells stably expressing an empty neomycin

resistant vector (Neo) or a DNp38 (Fig. 1*A*; ref. 9). The genes changing in expression in these treatments were grouped into two sets: a low-stringency set, which changed significantly in any of the three treatments (15); and a high-stringency set in which gene expression changed significantly in all of the three treatments.

So that we could identify TFs responsible for the p38-regulated growth arrest program, we looked in both the high and low stringency sets for TFs whose activities might explain the observed expression changes (16). For this, we used a database in which associations between TFs and their target gene promoters are represented numerically with interaction scores (Supplementary Fig. S1; Fig. 1). For each combination of a TF, T, and gene, G, present on the array, we asked the following questions. First, were there known or potential binding sites for T in the promoter of G? If so, we summed the scores for these to use as a "coregulation score" (Supplementary Fig. S1). Next, we asked if the expression change of *T* correlated with that of *G*. We took the nonparametric Spearman correlation between *T* and *G* across all samples as our "coexpression score" (Supplementary Fig. S1). Finally, we multiplied the coregulation and coexpression scores together to obtain a combined score. The magnitude of the combined score reflects the strength of the scores for both coregulation (i.e., if there are no binding sites for *T* upstream of *G*, the coregulation score and the product overall score will be zero) and coexpression (i.e., low correlations will be weighted proportionally lower). The sign of the combined score reflects correlation or anticorrelation, which by extension corresponds to potential transcriptional induction or repression (see Materials and Methods and Supplementary Fig. S1). We used a combined score threshold of 0.75, restricting genes to the high-stringency set, and restricting TFs to the low-stringency set to keep the networks manageable.

The low-stringency set (Supplementary Fig. S3) revealed an association network containing 129 genes. Of these 43 represent known TFs (*boxes*), the remainder correspond to other non-TF genes (*circles*; Supplementary Fig. S3; Fig. 1*B*). In the high-stringency set (Benjamini-Hochberg corrected test $P < 0.05$ in all treatments), 16 TFs were found to be consistently changing in expression (up, red; down, green) and correlation levels across the three strategies. Some of these (e.g., c-Jun, FoxM1, BHLHB3, and NR2F1; see below) seem to be connected to a larger number of target genes (Supplementary Fig. S3; Fig. 1*B*). We found that the majority of the genes regulated by p38 were similarly regulated between T-HEp3 and D-HEp3 cells (not shown). Thus, the p38-regulated genes are also changing during the reprogramming of tumorigenic to dormant phenotypes of HEp3 cells. Using the high-stringency set, we obtained a TF network amenable for experimental testing (Fig. 1). Nodes in this network included *c-Jun* and *FoxM1*, as genes negatively regulated by p38 signaling. In contrast, p38 induced the tumor suppressor p53, the transcriptional repressors *Nr2f1* (17), and the basic helix loop helix TF *BHLHB3/Dec2/Sharp-1* (18), two genes of relatively unknown function in cancer and not previously linked to p38. Next, we determined whether these findings were predictive of TF function in p38-induced quiescence of D-HEp3 cells. We selected four TFs, BHLHB3, c-Jun, p53, and FOXM1 for our initial analysis (see below), either because they were known targets of p38 (e.g., p53 and c-Jun) or because they were new targets not previously implicated in p38-mediated inhibition of tumor cell proliferation.

BHLHB3 is required for D-HEp3 cell quiescence and is regulated by ERK and p38. BHLHB3 is a clock gene (19, 20), a transcriptional repressor (18), and importantly, a tumor suppressor in lung cancer (21). In D-HEp3 cells, BHLHB3 is induced by p38 and was positively linked to genes involved in extracellular matrix biology (e.g., collagen-I α1, matrix metalloproteinase 2; Fig. 1*B*). Its induction by p38 suggested a role in tumor cell quiescence. T-HEp3 cells express less BHLHB3 mRNA than D-HEp3 cells and inhibition of p38 by SB203580 reduced BHLHB3 expression in D-HEp3 cells (Fig. 2*A*). Inhibition of Mek1/2 with PD98059 up-regulated BHLHB3 mRNA expression in D-HEp3 cells but to a lesser degree in T-HEp3 cells (Fig. 2*A*). We conclude that ERK and p38 signaling results in opposing regulation of BHLHB3 expression.

In D-HEp3 cells, siRNA targeting BHLHB3 resulted in a slightly stronger down-regulation of BHLHB3 to that obtained by a p38α siRNA as measured by RT-PCR and qPCR (Fig. 2*B*). SiRNA to p53 did not affect BHLHB3 expression (Fig. 2*B*), suggesting that its expression is not downstream of p53. Upon inoculation *in vivo*, we observed that like p38α knock-down, down-regulation of BHLHB3 also restored proliferation of D-HEp3 cells *in vivo* (Fig. 2*B*). We also tested D-HEp3 stably transduced with a different shRNA to BHLHB3 or a shRNA to luciferase or an empty vector (Fig. 2*C*). Upon *in vivo* inoculation, D-HEp3 cells expressing a shRNA to BHLHB3 contained >6-fold more cells per tumor nodule than the tumors from control cells (Fig. 2*C*). The same cells inoculated in nude mice showed a statistically significant shortening in the dormancy period for D-HEp3 cells with BHLHB3 knockdown (Fig. 2*C*). In agreement, overexpression of BHLHB3 in T-HEp3 was able to significantly inhibit their proliferation (Fig. 2*D*). This effect could be further enhanced by coexpression of an MKK6 active mutant that activates p38α (Fig. 2*D*; ref. 7). We conclude that BHLHB3 is a novel negative regulator of tumor growth functionally linked to p38 signaling.

Down-regulation of FoxM1 or c-Jun inhibits T-HEp3 growth *in vivo*. We next tested whether FoxM1 and c-Jun down-regulation by p38 was linked to D-HEp3 cell dormancy (Fig. 1). QPCR analysis revealed that c-Jun expression was higher in T-HEp3 than D-HEp3 cells (Fig. 3*A*). Furthermore, p38 inhibition resulted in c-Jun up-regulation only in D-HEp3 cells, whereas Mek1/2 inhibition down-regulated c-Jun expression in both cells (Fig. 3*A*). SiRNAs inhibition of c-Jun expression (Fig. 3*B*) did not affect BHLHB3 and FoxM1 mRNA levels (data not shown), suggesting that these genes are not downstream of c-Jun. However, c-Jun down-regulation by RNAi (si c-Jun-I) stimulated p53 expression in T-HEp3 cells and to some extent in D-HEp3 cells (Fig. 3*B*). Thus, our data support that p38-mediated up-regulation of p53 transcript is at least in part mediated by a p38-dependent inhibition of c-Jun induction. In addition, RNAi to c-Jun was sufficient to cause a strong inhibition of T-HEp3 proliferation *in vivo* (Fig. 3*B*). This correlated with reduced proliferation marker phospho-Histone H3 staining in siRNA-treated tumors, but not with increased apoptosis as measured by cleaved-caspase3 staining (Fig. 3*C*).

FoxM1 expression was repressed by p38 as SB203580 treatment up-regulated FoxM1 mRNA in D-HEp3 cells (Fig. 3*D*). RNAi-mediated down-regulation of FoxM1 was detected by RT-PCR and qPCR (Fig. 3*D*) and was also very efficient in inhibiting T-HEp3 tumor growth *in vivo* (Fig. 3*D*). Reduced tumor growth was also associated with reduced phospho-H3 levels in these tumors. However, inhibition of FoxM1 expression induced apoptosis by ~2-fold in T-HEp3 cells (Fig. 3*C*). We conclude that both FoxM1 and c-Jun are important to promote T-HEp3 tumor growth (and survival in the case of FoxM1).

Opposing regulation of $p53^{mutR213Q}$ by ERK and p38 contributes to D-HEp3 tumor cell quiescence. In D-HEp3 cells, p38 induced p53 mRNA (Fig. 1), which is in agreement with lower

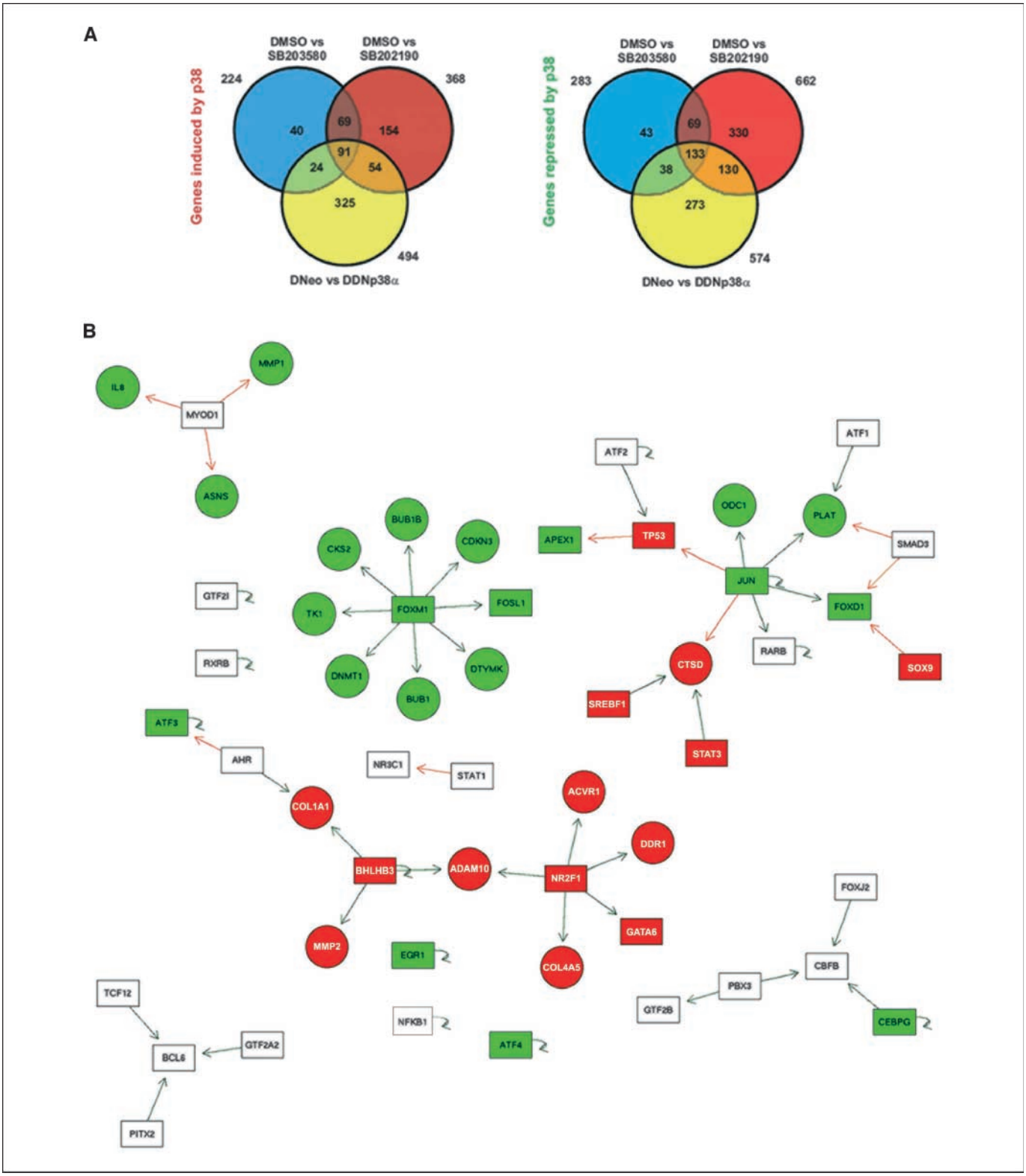

Figure 1. *A,* Venn diagrams of genes changing significantly (91 up, 133 down) to each of the three strategies using both the gcRMA and MAS5 methods. Significance was established with a *P* value of the F-statistic at 0.05. Total number of genes induced or repressed by p38 are indicated outside the Venn diagram. *B,* TF network regulated by p38 signaling showing only genes that move significantly up or down in all three of the p38 inhibition experiments and the TFs that potentially control them. *Boxes,* TFs; *circles,* target genes other than TFs. The colors indicate whether they were up-regulated (*red*) or down-regulated (*green*) by p38 signaling. Where a gene's promoter contains known/predicted binding sites for a given TF, the binding sites scores are summed and multiplied by their expression correlation (Spearman across all samples). An arrow is then drawn between the TF and gene where the score exceeds a threshold of 0.75. Arrow colors indicate whether the genes were negatively (*orange*) or positively (*green*) coregulated. *White boxes,* changes in TF expression that were not statistically significant but still were significantly correlated with the putative target genes. The expression level trend of white box TFs can be inferred by the color of the connecting arrow.

p53 mRNA level in tumor versus normal head and neck cancer tissue (Supplementary Fig. S4; ref. 22). Furthermore, in ~50% of head and neck squamous cell carcinomas (HNSCC), p53 is mutated (23). Indeed, we found in both T- and D-HEp3 cells a mutation comprising an Arg to Gln substitution at codon 213 (R213Q; Fig. 4), which is present in oral cancers (24). Sequencing data in Supplementary Fig. S5 showed that the CGA to CAA G->A substitution seems to be complete suggesting that both alleles are mutated. Although mutations or posttranslational modifications can inactivate p53, we tested whether $p53^{mutR213Q}$ was functional in HEp3 cells and whether transcriptional down-regulation of $p53^{mutR213Q}$ may be an additional mechanism to overcome p53 inhibitory effects.

As shown in Fig. 4, p53 mRNA and protein levels were up-regulated in D-HEp3 versus T-HEp3 cells. Basal luciferase reporter expression driven by a p53-binding element was 6- to 10-fold higher in D-HEp3 than T-HEp3 cells (Supplementary Fig. S5), suggesting a functional p53 protein despite the R213Q mutation. SB203580 (10 μmol/L) treatment, which almost completely reduces Hsp27 phosphorylation by p38α/β, although p38γ and p38δ are also expressed (Supplementary Fig. S5), inhibited p53 mRNA (48 hours), protein expression, and activity (Supplementary Fig. S5; Fig. 4) in D-HEp3 cells. Also, Mek1/2 inhibition caused a dramatic up-regulation in p53 mRNA and activity in both cells (Supplementary Fig. S5; Fig. 4). In addition, phosphorylation of p53 at Ser15 after modulation of ERK or p38 activity and protein turnover following proteasome inhibition were unaffected in T-HEp3 and D-HEp3 cells (data not shown). Endogenous p53 protein level and activity could be induced by doxorubicin in T-HEp3 and D-HEp3 cells albeit to a lesser extent in the latter (Supplementary Fig. S5). However, the

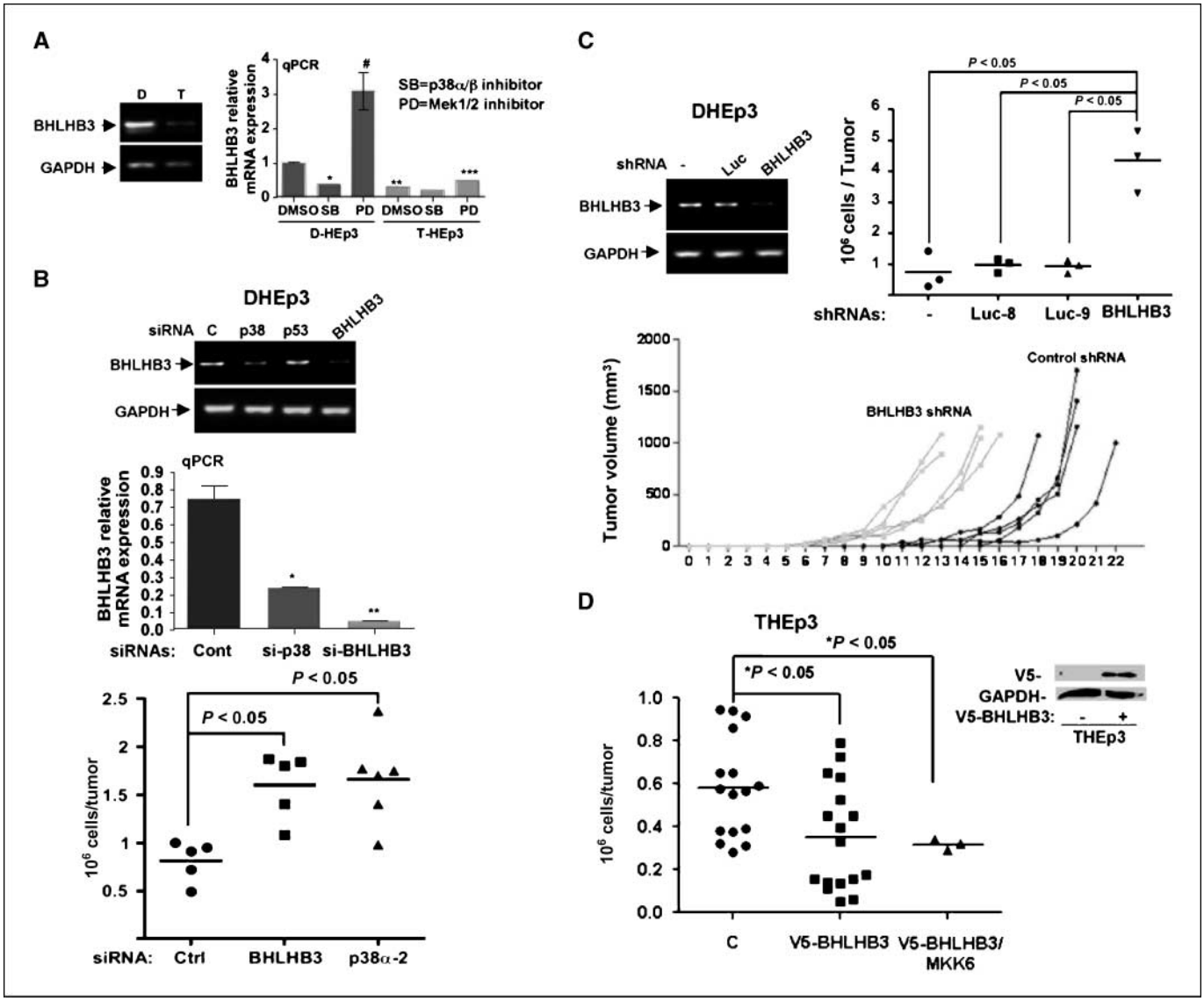

Figure 2. BHLHB3 is required for D-HEp3 cell quiescence. *A,* basal expression of BHLHB3 detected by RT-PCR (*left*) or (*right*) qPCR under the indicated treatments for 24 h. *PD,* 20 μmol/L PD98059 Mek1/2 inhibitor; *SB,* 10 μmol/L SB203580 p38 inhibitor; *DMSO,* DMSO used as vehicle. *B,* siRNA-mediated knockdown of BHLHB3 or p38α, but not p53, caused a strong decrease in BHLHB3 mRNA as measured by RT-PCR (*top*) or qPCR (*middle*) and interrupts the quiescence of D-HEp3 cells (*bottom*). *C,* shRNA stable knockdown of BHLHB3 measured by RT-PCR (*left*) not observed with shRNAs to luciferase (*Luc*) results in restored proliferation of D-HEp3 cells *in vivo* (*right*). *Bottom,* when inoculated in nude mice (2×10^5 cells/mouse), D-HEp3 cells expressing BHLHB3 shRNA have a statistically significant shortening in their dormancy period. *D,* overexpression of V5-BHLHB3 inhibits proliferation of T-HEp3 cells on CAMs *in vivo* (*left*). *Right,* detection of the V5-tag after transfection of T-HEp3 cells with an empty vector or V5-BHLHB3. MKK6 is not tagged and its expression has been verified (21).

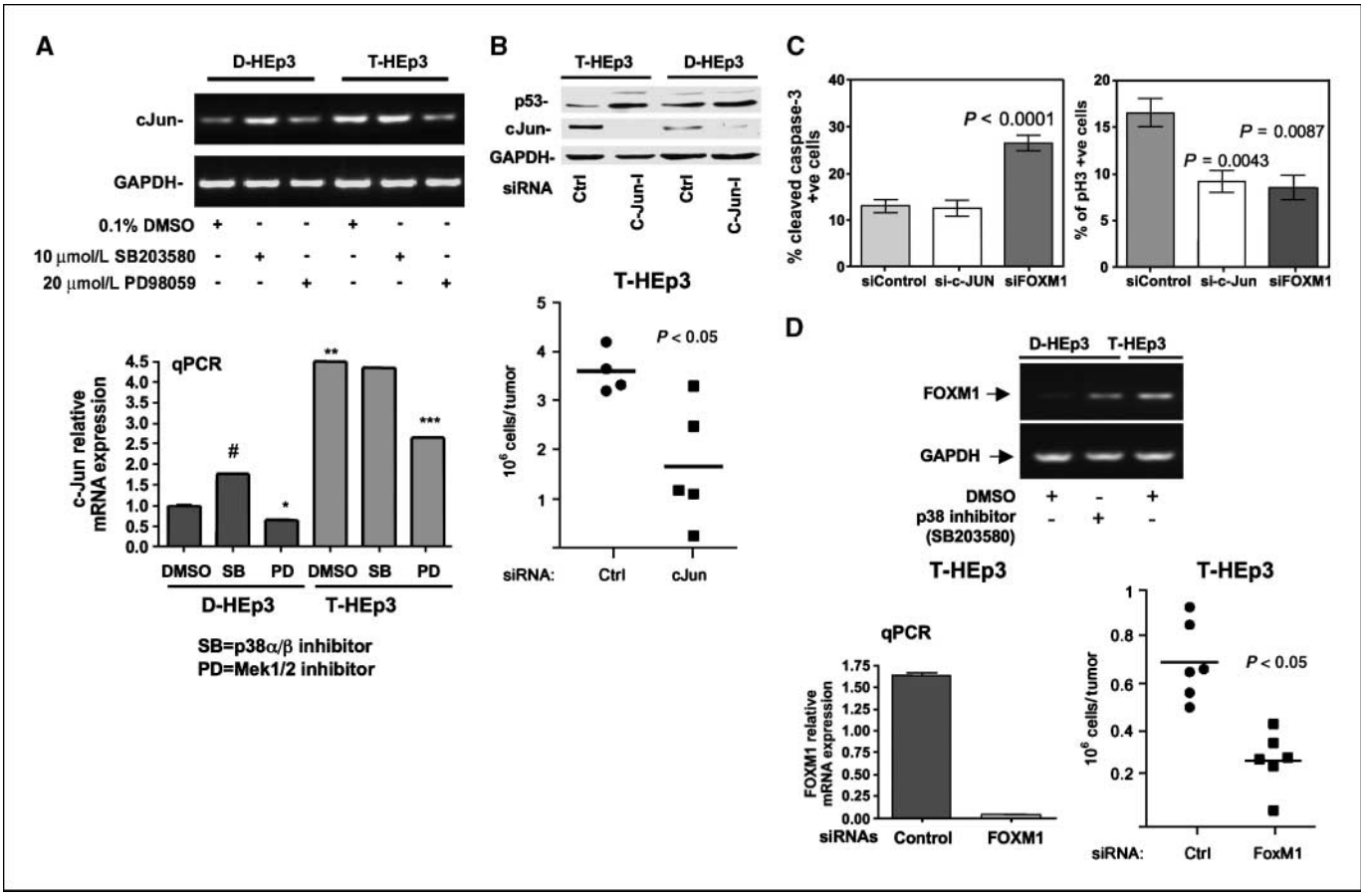

Figure 3. *A,* basal c-Jun expression is lower in D-HEp3 cells than in T-HEp3 cells, increased by 10 μmol/L SB203580 (*SB*) treatment in D-HEp3 cells and reduced by 20 μmol/L PD98059 (*PD*) in T-HEp3 cells as measured by RT-PCR (*top*) and qPCR (*middle*). *B,* siRNA-mediated down-regulation of c-Jun detected by Western blot (*top*) reduced cell proliferation of T-HEp3 cells after 4 d *in vivo* (*bottom*). Scrambled siRNAs served as controls. *C,* quantification of apoptosis (cleaved caspase-3 staining) in 2-d-old tumors of T-HEp3 cells transfected with control, c-Jun, or FoxM1 siRNAs (*left*). *Right,* quantification of phospho-histone H3 levels in the same samples (triplicate experiments). *D,* basal (DMSO) FoxM1 expression level is lower in D-HEp3 cells than in T-HEp3 cells and can be induced by 10 μmol/L SB203580 (*SB*) treatment in D-HEp3 cells (*top*). siRNA-mediated knockdown of FoxM1 for 48 h, as detected by qPCR (*bottom*), reduced cell expansion of T-HEp3 cells after 3 d *in vivo* (*bottom*).

downstream target Bax was induced poorly in T-HEp3 cells and did not change in D-HEp3 cells, which have high basal p53 and Bax expression (Supplementary Fig. S5). Marginal Bax induction is in agreement with the abrogated capacity of the R123Q p53 mutant to induce apoptotic genes (24). Finally, p53 activity was significantly higher in D-HEp3 cells compared with T-HEp3 cells after 3 days *in vivo*. This suggests that higher $p53^{mutR213Q}$ expression and activity in D-HEp3 cells persists upon *in vivo* growth arrest (Fig. 4) and that this mutant p53 may allow HNSCC cells to uncouple growth arrest from apoptosis in response to stress.

We next tested whether p53 is required for p38-induced quiescence via RNAi. The shRNAs to p53 showed a consistent and specific down-regulation of p53 protein of approximately 50% to 60% (Fig. 4*C*) compared with a shRNA to luciferase. SiRNAs to p53 targeting a different region of the mRNA generated an almost complete reduction in mRNA and protein after 48 hours by qPCR and Western blot, respectively (Fig. 4*D*). In all instances, down-regulation of p53 was sufficient to allow these cells to resume proliferation *in vivo* (Fig. 4*C* and *D*). These results further support the predictive value of the TF network and suggest that $p53^{mutR213Q}$ is in part required for p38-induced quiescence in D-HEp3 cells.

Discussion

We have identified a gene expression program responsible for p38-induced tumor cell quiescence and the TFs executing this program by using computational tools that (*a*) revealed TF networks, (*b*) were predictive of gene function, and (*c*) were of a complexity level addressable experimentally. Our analysis identified p38 coregulated targets were functionally linked to the quiescent phenotype of D-HEp3 cells. Furthermore, we revealed clues about the activating or repressing functions of several TFs (present in TRANSFAC) on numerous gene promoters.

Our analysis identified TFs potentially responsible for the quiescent phenotype of D-HEp3 cells that could be validated *in vivo.* For example, inhibiting p53 and BHLHB3 resulted in a similar phenotype to that of p38 inhibition. BHLHB3 and p53 seem to have similar abilities to suppress growth despite the apparent difference in the number of predicted downstream targets in the network. This also suggests that the number of connected genes may not directly assign phenotypic importance to a TF. It was noticeable that for c-Jun and FoxM1 or Nr2F1 and BHLHB3, although clearly coregulated by p38, there was no single common regulating TF. Identification of p38 target genes *in vivo* where D-HEp3 cells fully growth arrest (25) and/or temporal studies will

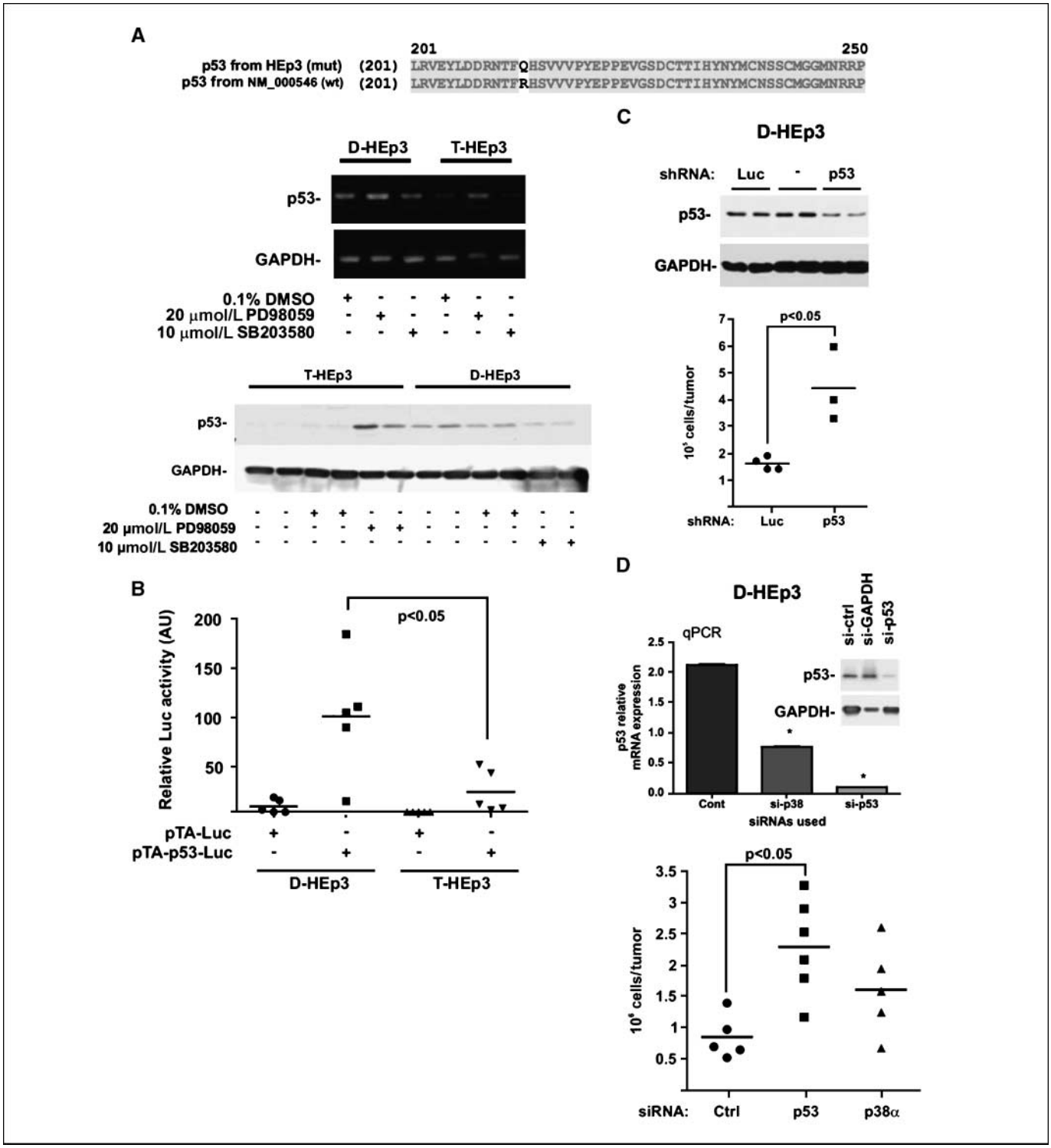

Figure 4. *A,* protein sequence alignment along aa 201 to 250 between wt (NM_000546) and mutant p53 in HEp3 cells shows an R213Q substitution (*top*). Basal p53 mRNA (*middle*) and protein (*bottom*) expression is higher in D-HEp3 cells than in T-HEp3 cells; *lanes,* treatments with vehicle (DMSO) or Mek1/2 inhibitor PD98059 (20 μmol/L) or p38 inhibitor SB203580 (10 μmol/L), as measured by RT-PCR and Western blot, respectively. *B,* p53 luciferase reporter activity measured *in vivo* was higher in D-HEp3 cells than T-HEp3 cells after 72 h *in vivo* growth on CAMs. *C,* shRNA knockdown of p53 measured by Western blot (*top*), results in restored proliferation of D-HEp3 cells *in vivo* (*bottom*). *D,* knockdown of p53 by siRNAs in DHEp3 cells was measured at the protein level by Western blot and qPCR (*top*), and promoted cell proliferation *in vivo* in D-HEp3 cells (*bottom*). All experiments performed at least in triplicate.

help identify additional p53 targets and upstream regulators of these TFs.

We found that p38-induced D-HEp3 cell quiescence required down-regulation of c-Jun, which is consistent with its role in G_1-S transition (26) and the up-regulation in tumor versus normal HNSCC tissue (Supplementary Fig. S4*B*). Accordingly, recent data showed that p38α deficient mouse fetal livers strongly up-regulated c-Jun and resulted in accelerated liver cancer development (5).

Similar results were observed in mice lacking p38α in the lung (4). We found that the up-regulation of p53 by p38 required down-regulation of c-Jun, as its knockdown was sufficient to induce p53 and inhibit T-HEp3 tumorigenesis (Fig. 3*B*). The antagonistic effect of c-Jun on p53 was shown to be linked to p38α signaling in liver regeneration (27) and mouse liver cancer development (28). Furthermore, c-Jun−/− mouse embryo fibroblasts (MEFs) have a proliferative defect mostly attributed to the transcriptional up-regulation of p53, which was dependent on c-Jun–mediated transcriptional repression from PF-1 site on p53 promoter (29). Similarly, blocking FoxM1 in T-HEp3 cells inhibited their growth *in vivo*. Still, this was linked to reduced proliferation and to a 2-fold increase in apoptosis, suggesting that in D-HEp3 cells, down-regulation of FoxM1 and the potential loss of prosurvival signaling might be compensated by other recently described survival pathways (30). FoxM1 is a known regulator of G_1-S and G_2-M transition and it is located at the 12p13 locus, which is usually amplified in HNSCC (31). Furthermore, the Oncomine database shows that FoxM1 transcript is up-regulated in HNSCC versus normal tissues (Supplementary Fig. S4C; ref. 32), and if expressed at high levels in primary breast tumors, it might be a poor prognosis indicator (33, 34). Our results suggest that reprogramming by p38 of D-HEp3 cells requires decreased FoxM1 and c-Jun expression to enter prolonged G_0-G_1 arrest *in vivo*.

Transcriptional regulation of p53 was important for p38-induced D-HEp3 cell quiescence. This was interesting because T- and D-HEp3 cells carry an R213Q mutation in p53. We show that $p53^{mutR213Q}$ can still induce quiescence and that it is regulated by p38 (1, 35). Our data diverged from other studies on posttranslational regulation of p53 (1, 35), in that ERK and p38 had opposing roles in the regulation of p53 at the transcript level. The Oncomine data supports that transcriptional down-regulation of p53 occurs in patients (Supplementary Fig. S4*A*; ref. 22). This suggests that spontaneous reprogramming and quiescence in HNSCC might occur upon up-regulation of p53 even in patients displaying the $p53^{mutR213Q}$. Thus, this mutation might predict for dormant disease as it may eliminate p53 proapoptotic functions (24) but allows tumor cells to enter quiescence. This may be due to the inability of codon 213 mutants to bind the p53 binding proteins ASPP1/2, which stimulate p53 to *trans*-activate apoptosis but not growth arrest genes (36, 37).

Another required component that seems to operate in parallel to p53 is BHLHB3. This transcriptional repressor is very important for p38-induced D-HEp3 cell quiescence and we are currently dissecting the mechanisms by which it induces tumor cell dormancy. BHLHB3 is expressed at higher levels in tumor versus normal HNSCC tissues (Supplementary Fig. S4*D*), suggesting that in the primary tumor, BHLHB3 expression may vary between different cancer types. However, the Oncomine database contains studies showing that high expression of BHLHB3 in primary breast cancer tumors is a good prognosis indicator (33, 34). In agreement, while this article was under review, Adorno and colleagues (38) showed that BHLHB3 is a transforming growth factor (TGF)β target gene down-regulated in breast carcinoma cells that bear a p53R175H mutation that blocks p63 function. Consequently they found that *BHLHB3* serves as a metastasis suppressor gene and that its down-regulation was associated with poor prognosis in breast cancer (38). However, a mechanism was not described. We speculate that induction of quiescence and consequently metastatic dormancy dependent on p38 and BHLHB3, both targets of TGFβ signaling (38–40), may be responsible for the metastasis suppression observed by Adorno and colleagues (38). We also showed that the ERK/p38 ratio is predictive of dormancy/quiescence of fibrosarcoma, breast, prostate, and squamous carcinoma cell lines (7–9) and similar results were observed with cervical carcinoma HeLa cells (11). Thus, collectively, our findings in this model of HNSCC quiescence might reveal important mechanisms driving dormancy and subsequent metastatic growth in different types of cancer.

Our studies reveal a previously unrecognized network of TFs regulated by p38 and required for the induction of tumor cell quiescence. Understanding how these TFs contribute to p38-induced growth arrest is of importance because inhibiting and/or reactivating more than one gene may be required to inhibit tumor progression. The strategy presented here may help identify new therapeutic targets or prognostic indicators when applied to large array data sets from patient samples.

Disclosure of Potential Conflicts of Interest

No potential conflicts of interest were disclosed.

Acknowledgments

Received 10/14/08; revised 5/8/09; accepted 5/21/09; published OnlineFirst 7/7/09.

Grant support: NIH/National Cancer Institute grant CA109182 (J.A. Aguirre-Ghiso), the U.S. Army Medical Research Acquisition Activity W8IWXH-04-1-0474 (D.S. Conklin), and by the Samuel Waxman Cancer Research Foundation Tumor Dormancy Program (J.A. Aguirre-Ghiso and D.S. Conklin). A.C. Ranganathan is a recipient of a Ruth L. Kirschstein National Research Service Award (NIH/ National Cancer Institute) Fellowship. D.M. Schewe is a recipient of a Dr. Mildred-Scheel postdoctoral grant by the Deutsche Krebshilfe.

The costs of publication of this article were defrayed in part by the payment of page charges. This article must therefore be hereby marked *advertisement* in accordance with 18 U.S.C. Section 1734 solely to indicate this fact.

We acknowledge the help of Drs. Thomas Begley (SUNY-Albany), Ari Melnick (Cornell University), and Yang Zheng (MSSM).

References

1. Bulavin DV, Fornace AJ, Jr. p38 MAP kinase's emerging role as a tumor suppressor. Adv Cancer Res 2004;92:95–118.
2. Bulavin DV, Demidov ON, Saito S, et al. Amplification of PPM1D in human tumors abrogates p53 tumor-suppressor activity. Nat Genet 2002;31:210–5.
3. Bulavin DV, Phillips C, Nannenga B, et al. Inactivation of the Wip1 phosphatase inhibits mammary tumorigenesis through p38 MAPK-mediated activation of the p16(Ink4a)-p19(Arf) pathway. Nat Genet 2004;36:343–50.
4. Ventura JJ, Tenbaum S, Perdiguero E, et al. p38α MAP kinase is essential in lung stem and progenitor cell proliferation and differentiation. Nat Genet 2007;39:750–8.
5. Hui L, Bakiri L, Mairhorfer A, et al. p38α suppresses normal and cancer cell proliferation by antagonizing the JNK-c-Jun pathway. Nat Genet 2007;39:741–9.
6. Junttila MR, Ala-Aho R, Jokilehto T, et al. p38α and p38δ mitogen-activated protein kinase isoforms regulate invasion and growth of head and neck squamous carcinoma cells. Oncogene 2007;26:5267–79.
7. Aguirre-Ghiso JA, Estrada Y, Liu D, Ossowski L. ERK(MAPK) activity as a determinant of tumor growth and dormancy; regulation by p38(SAPK). Cancer Res 2003;63:1684–95.
8. Aguirre-Ghiso JA, Ossowski L, Rosenbaum SK. Green fluorescent protein tagging of extracellular signal-regulated kinase and p38 pathways reveals novel dynamics of pathway activation during primary and metastatic growth. Cancer Res 2004;64:7336–45.
9. Aguirre-Ghiso JA, Liu D, Mignatti A, Kovalski K, Ossowski L. Urokinase receptor and fibronectin regulate the ERK(MAPK) to p38(MAPK) activity ratios that determine carcinoma cell proliferation or dormancy *in vivo*. Mol Biol Cell 2001;12:863–79.
10. Hickson JA, Huo D, Vander Griend DJ, et al. The p38 kinases MKK4 and MKK6 suppress metastatic colonization in human ovarian carcinoma. Cancer Res 2006;66:2264–70.
11. Timofeev O, Lee TY, Bulavin DV. A subtle change in p38 MAPK activity is sufficient to suppress *in vivo* tumorigenesis. Cell Cycle 2005;4:118–20.
12. Ossowski L, Reich E. Changes in malignant phenotype of a human carcinoma conditioned by growth environment. Cell 1983;33:323–33.
13. Liu D, Aguirre Ghiso J, Estrada Y, Ossowski L. EGFR is

a transducer of the urokinase receptor initiated signal that is required for *in vivo* growth of a human carcinoma. Cancer Cell 2002;1:445–57.
14. Ranganathan AC, Ojha S, Kourtidis A, Conklin DS, Aguirre-Ghiso JA. Dual function of pancreatic endoplasmic reticulum kinase in tumor cell growth arrest and survival. Cancer Res 2008;68:3260–8.
15. Smyth GK. Linear models and empirical bayes methods for assessing differential expression in microarray experiments. Stat Appl Genet Mol Biol 2004;3: Article3.
16. Tuck DP, Kluger HM, Kluger Y. Characterizing disease states from topological properties of transcriptional regulatory networks. BMC Bioinformatics 2006;7:236.
17. Ferrer-Martinez A, Marotta M, Baldan A, Haro D, Gomez-Foix AM. Chicken ovalbumin upstream promoter-transcription factor I represses the transcriptional activity of the human muscle glycogen phosphorylase promoter in C2C12 cells. Biochim Biophys Acta 2004;1678:157–62.
18. Azmi S, Ozog A, Taneja R. Sharp-1/DEC2 inhibits skeletal muscle differentiation through repression of myogenic transcription factors. J Biol Chem 2004;279: 52643–52.
19. Kawamoto T, Noshiro M, Furukawa M, et al. Effects of fasting and re-feeding on the expression of Dec1, Per1, and other clock-related genes. J Biochem (Tokyo) 2006;140:401–8.
20. Rohleder N, Langer C, Maus C, et al. Influence of photoperiodic history on clock genes and the circadian pacemaker in the rat retina. Eur J Neurosci 2006;23: 105–11.
21. Falvella FS, Colombo F, Spinola M, et al. BHLHB3: a candidate tumor suppressor in lung cancer. Oncogene 2008;27:3761–4.
22. Toruner GA, Ulger C, Alkan M, et al. Association between gene expression profile and tumor invasion in oral squamous cell carcinoma. Cancer Genet Cytogenet 2004;154:27–35.
23. Gath HJ, Brakenhoff RH. Minimal residual disease in head and neck cancer. Cancer Metastasis Rev 1999;18: 109–26.
24. Pan Y, Haines DS. Identification of a tumor-derived p53 mutant with novel transactivating selectivity. Oncogene 2000;19:3095–100.
25. Aguirre Ghiso JA, Kovalski K, Ossowski L. Tumor dormancy induced by downregulation of urokinase receptor in human carcinoma involves integrin and MAPK signaling. J Cell Biol 1999;147:89–104.
26. Nicolaides NC, Correa I, Casadevall C, et al. The Jun family members, c-Jun and JunD, transactivate the human c-myb promoter via an Ap1-like element. J Biol Chem 1992;267:19665–72.
27. Stepniak E, Ricci R, Eferl R, et al. c-Jun/AP-1 controls liver regeneration by repressing p53/p21 and p38 MAPK activity. Genes Dev 2006;20:2306–14.
28. Eferl R, Ricci R, Kenner L, et al. Liver tumor development. c-Jun antagonizes the proapoptotic activity of p53. Cell 2003;112:181–92.
29. Schreiber M, Kolbus A, Piu F, et al. Control of cell cycle progression by c-Jun is p53 dependent. Genes Dev 1999;13:607–19.
30. Schewe DM, Aguirre-Ghiso JA. ATF6α-Rheb-mTOR signaling promotes survival of dormant tumor cells *in vivo*. Proc Natl Acad Sci U S A 2008; 105:10519–24.
31. Laoukili J, Stahl M, Medema RH. FoxM1: at the crossroads of ageing and cancer. Biochim Biophys Acta 2007;1775:92–102.
32. Rhodes DR, Yu J, Shanker K, et al. ONCOMINE: a cancer microarray database and integrated data-mining platform. Neoplasia 2004;6:1–6.
33. van 't Veer LJ, Dai H, van de Vijver MJ, et al. Gene expression profiling predicts clinical outcome of breast cancer. Nature 2002;415:530–6.
34. van de Vijver MJ, He YD, van't Veer LJ, et al. A gene-expression signature as a predictor of survival in breast cancer. N Engl J Med 2002;347:1999–2009.
35. Bulavin DV, Saito S, Hollander MC, et al. Phosphorylation of human p53 by p38 kinase coordinates N-terminal phosphorylation and apoptosis in response to UV radiation. EMBO J 1999;18:6845–54.
36. Samuels-Lev Y, O'Connor DJ, Bergamaschi D, et al. ASPP proteins specifically stimulate the apoptotic function of p53. Mol Cell 2001;8:781–94.
37. Thukral SK, Blain GC, Chang KK, Fields S. Distinct residues of human p53 implicated in binding to DNA, simian virus 40 large T antigen, 53BP1, and 53BP2. Mol Cell Biol 1994;14:8315–21.
38. Adorno M, Cordenonsi M, Montagner M, et al. A Mutant-p53/Smad complex opposes p63 to empower TGFβ-induced metastasis. Cell 2009;137:87–98.
39. Cocolakis E, Lemay S, Ali S, Lebrun JJ. The p38 MAPK pathway is required for cell growth inhibition of human breast cancer cells in response to activin. J Biol Chem 2001;276:18430–6.
40. Gal A, Sjoblom T, Fedorova L, et al. Sustained TGF β exposure suppresses Smad and non-Smad signalling in mammary epithelial cells, leading to EMT and inhibition of growth arrest and apoptosis. Oncogene 2008;27: 1218–30.